

PV Maximum Power-point Tracking Using Modified Particle Swarm Optimization under Partial Shading Conditions*

Al-wesabi Ibrahim^{1,2}, *M.B. Shafik*^{3*}, *Min Ding*^{1,2}, *Mohammad Abu Sarhan*^{1,2}, *Zhijian Fang*^{1,2},
*Ahmed. G. Alareqi*⁴, *Tariq Al'moqri*⁵ and *Ayman. M. Al-Rassas*⁶

(1. School of Automation, China University of Geoscience, Wuhan 430074, China;

2. Hubei Key Laboratory of Advanced Control and Intelligent Automation for Complex Systems, Wuhan 430074, China;

3. School of Electrical Engineering and Automation, Wuhan University, Wuhan 430072, China;

4. School of Oil and Natural Gas Engineering, China University of Geosciences, Wuhan 430074, China;

5. School of Mathematics and Physics, China University of Geoscience, Wuhan 430074, China;

6. School of Petroleum Engineering, China University of Petroleum, East China, Qingdao 266580, China)

Abstract: A novel maximum power-point tracking approach is proposed based on studies investigating the output characteristics of photovoltaic (PV) systems under partial shading conditions. The existence of partially shaded conditions leads to the presence of several peaks on PV curves, which decrease the efficiency of conventional techniques. Hence, the proposed algorithm, which is based on the modified particle-swarm optimization (MPSO) technique, increases the output power of PV systems under such abnormal conditions and has a better performance compared to other methods. The proposed method is examined under several scenarios for partial shading condition and non-uniform irradiation levels using Matlab, and to investigate its effectiveness adequately, the results of the proposed method are compared with those of the neural network technique. The experimental results show that the proposed method can decrease the interference of the local maximum power-point to cause the PV system to operate at a global maximum power-point. The efficiency of the MPSO is achieved with the least number of steady-state oscillations under partial shading conditions compared with the neural network method.

Keywords: Photovoltaic(PV), maximum power point tracking(MPPT), step-up converter, artificial neural networks (ANNs), particle-swarm optimization (PSO)

1 Introduction

The sustainability of solar energy and the resulting reduction in its material cost has led to the widespread application of photovoltaic (PV) systems in daily lives. However, during the practical implementation of PV systems, their short life cycles and low energy efficiency are the main associated

problems. The main reasons for this are the power loss and hot-spots, which are caused by the presence of partial shadows.

Under uniform irradiation levels, the tracking process of the maximum power-point of PV systems based on classical strategies can have a suitable performance. However, if a PV system operates under a partial shading condition (PSC), the power-voltage (P-V) characteristic curve of the PV system will have different local maximum points resulting from the connection of bypass diodes to reduce the impact of hot-spots.

The existence of several peaks on the PV characteristic curve increases the complexity associated with the extraction of the global maximum

Manuscript received June 6, 2020; revised July 29, 2020; accepted November 19, 2020.
Date of publication December 31, 2020; date of current version December 10, 2020.

* Corresponding Author, E-mail: muhammedshafiq@yahoo.com

* Supported by the Hubei Provincial Natural Science Foundation of China (2015CFA010), the Technology Project of State Grid Company "Soft Connection Mechanism and Modeling of Smart Grid Adapting to the Development of Global Energy Interconnection," and the 111 Projects (B17040).

point under these conditions, and there is a need to propose a more suitable control system that can distinguish between local and global maxima to ensure the maximum possible power, thus enhancing the total system efficiency. For this reason, the key purpose of this study is to propose an intelligent maximum power-point tracking (MPPT) tracker that enables the efficient prediction of the global maximum power-point (GMPP) from a PV system, regardless of the condition of the surrounding atmosphere, whether under uniform or non-uniform solar irradiation levels.

In the literature, several global MPP search algorithms have been developed to determine the global MPP under conditions of partial shading.

The attempt to deal with such a difficulty has been reported in a few papers. Furthermore, a large number of these methods have some disadvantages, such as their complexity, difficult implementation, high cost, and the need for multiple measured parameters. A straightforward MPPT method using the Fibonacci line search has been observed in Ref. [1]. In this method, the research limit is moved repeatedly to benefit from the best advantage of the search limit, which can track the MPP under the condition of uniform irradiation or stable change of irradiation. However, it is difficult to extract the global peak under local shading and harsh environmental conditions. In Ref. [2], the authors designed a three-layer feed-forward artificial neural network (ANN) with a controller based on polar information for the global point tracking of partially shaded solar arrays. However, the results of this method were accompanied by some drawbacks, such as the excessive complexity of the control scheme and a large number of computations. In Refs. [3-4] a tracking method was proposed to determine the maximum power using both simulation software and hardware implementation. This method is based on particle swarm optimization (PSO), which extracts the global peak (GP) in the case of partial shadows to boost the output power of the solar system. This technique catches and finds the GMPP under various climate circumstances, but the global peak should be distinguished via the features of the output PV array. Therefore, the function must be converted by the output PV array curves, and the PSO algorithm is then applied to obtain the global optimal

solution. Therefore, under any rapid variation of irradiation level or partial shading, there will be a large number of computations and tracking times. All the previously mentioned methods have been designed with less intensive non-uniform irradiation levels and partial shading. In addition, these methods have common weaknesses, such as slow tracking speed, the need for training, and obtaining the local optimum.

In Ref. [5], a new metaheuristic algorithm is proposed, namely the adaptive radial movement optimization (AMRO), to overcome the output problems of PV systems under the PSC, and the working process of AMRO is very similar to that of RMO. However, in the whole process of the algorithm, the coefficients in the AMRO will change adaptively. AMRO starts the optimization process by scattering multiple particles in a predefined search space. The scattered particles are then used as a proposed solution. Therefore, the main difference between AMRO and other optimization methods is the motion mode of particles. AMRO can be the MPPT control unit to track the GMPP under the PSC. A differential evolution (DE) optimization algorithm is proposed in Ref. [6] to track and capture the precise GMPP that is executed by a single-ended primary inductor converter (SEPIC). The result is fast convergence to GMPP. Ref. [7] focuses on the performance evaluation and provides a detailed comparison for the most recent six works based on artificial intelligence technology, which can carry out MPPT according to the PSC.

In Refs. [8-12], modifications of conventional MPPT methods are proposed to improve the efficiency and performance of these methods, which is an improved P&O (MPPT) method based on the adaptive duty cycle step of fuzzy logic controllers^[8], and a new IC MPPT algorithm is proposed using direct control based on the fuzzy duty cycle change estimator^[9]. Some modifications to the IC method are proposed in Refs. [10-12] to extract the GMPP of PV systems under the PSC. Ref. [13] proposes a simple and fast convergence MPPT method that does not require additional control loops or intermittent links. The algorithm uses the relationship between the load line and I-V curve and combines with the triangle rule to obtain a fast response.

The PSO technique is a method that uses a

“swarm” of potential solutions to improve an optimal solution to the problem^[14]. With this method, the level of optimality is measured using a fitness function. The PSO is different from other methods of evolutionary computation so that members of the swarm, which are called “particles”, are dispersed in the space of the problem. This paper proposes MPSO and ANN algorithms to address the complex nonlinear problem of PV systems. Nowadays, heuristic algorithms (PSO) have been applied to resolve different engineering problems, such as: ① nonlinear optimization problems; ② training neural networks; ③ heating system planning; and ④ power systems. According to the investigation, the PSO technique is easy, effective, and robust, and it is a population-based algorithm that can be used to treat optimization problems. Some modifications are necessary to enhance the performance of PSO. Therefore, MPSO modifies the velocity step function, controls the velocity limit, and controls the search space, as presented in detail in Section 6. Therefore, this work determines the performance of the MPSO and ANN MPPT method under various solar irradiation conditions and PSCs.

Section 2 discusses the PV array model, and Sections 3 and 4 discuss PSC and the effect of the bypass diode, respectively. Section 5 explains the use of the DC-DC boost converter, while Section 6 presents the MPSO algorithm and application to MPPT. Section 7 discusses simulation results, and Section 8 presents the conclusions.

Significant contributions are incorporated in this work, and these are summarized as follows.

(1) A modified version of the particle swarm optimizer is proposed to enhance the performance of MPPT of PVs under the PSC.

(2) Modified particle swarm optimization (MPSO) is compared with an ANN in order to extract the true maximum energy from the PV panel at different radiation levels under PSCs.

2 Formulation of PV system

PV cells are a primary ingredient of solar power generation. They use PN junctions to generate a solar PV effect and convert solar energy into electricity. The output power of a single PV cell is small. However, in

actual applications, the desired power can be achieved once they form a PV array either in series or parallel. The output features of PV arrays are nonlinear and time-varying and are easily influenced by the incident light intensity, cell temperature, load conditions, and parasitic impedance, among other factors, resulting in solar energy utilization that cannot always be maximized^[15-16].

PV cells are made up of semiconductor material PN junctions that generate a direct voltage when receiving a PV light. They may be symbolized by a parallel connection of both a constant current source and forward diode. The equivalent electrical circuit of the solar PV cell is seen in Fig. 1, where I_{ph} is the photon-provided current, and its value depends on the light-receiving area of the PV cell, the illumination intensity of the incident light, and the surrounding temperature; I_D is the reverse current in the PV cell; I_{sh} is the shunt current that goes through the bypass resistor R_{sh} , and it is generated owing to the battery edge and metal bridge leakage on the metal electrode; R_s is the series-connected resistor, which is related to the contact resistance and the resistivity of the material itself; I_{pv} and V_{pv} are the solar PV current and voltage, respectively.

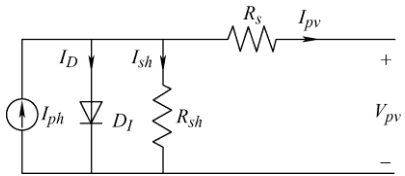


Fig. 1 Equivalent circuit of PV cell

To simulate the PV cell in Matlab/Simulink, the mathematical equation of the equivalent circuit output module is needed. Therefore, Kirchhoff's Current Law (KCL) is used to calculate the output current I_{pv} of PV cells, as shown in the following equation

$$I_{pv} = N_p I_{ph} - N_p I_o \left[\exp \left(\frac{q(V_{pv} + I_{pv} R_s)}{N_s A K T} \right) - 1 \right] - \left(\frac{V_{pv} + I_{pv} R_s}{R_{sh}} \right) \quad (1)$$

where V_{pv} is the solar cell voltage, R_s is the series-connected resistor, R_{sh} is the shunt resistance, q is the electron charge (1.6×10^{-19} C), N_s is the number of solar cells connected in series, N_p is the number of solar cells connected in parallel, I_o is the reverse saturation current under typical test conditions, T is the

degree of absolute temperature, A is the value of the diode ideality constant, and K is the Boltzmann constant (1.38×10^{-23} J/K).

3 Principle of partial shading

The shading of PV modules can be either partial or total owing to the movement of objects that can block the sunlight from the PV modules. As a result, the output attributes of solar modules are more complex with various peak points. The P-V curve of the shaded PV array has multiple local peaks, rather than only one peak for non-shaded PV arrays. Therefore, only the global peak can assure the highest power rather than the other different peaks. Global peaks and local peaks are shown in Figs. 2a-2b.

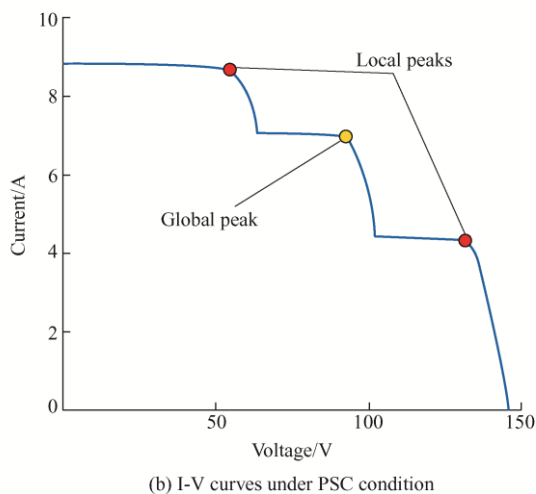
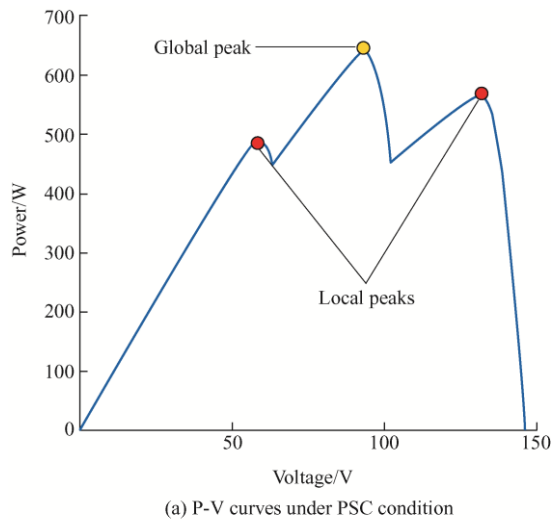


Fig. 2 P-V and I-V curves under PSC condition

The PV array may be defective owing to different

aging effects. These effects may also result from different outer reasons, which include dust, dirt, surrounding plants, and bird droppings, which cause partial or total shading conditions and increased internal temperature. Hence, these may be the reason for more optical and physical cell degradation phenomena.

At times, designers do not consider the shading effect, which can be easily ignored. For this reason, it is essential to perform detailed predictions of the solar resources, considering different factors such as the orientation, inclination, and potential shading by surrounding trees and buildings. In addition, the partial shading problem should be resolved by performing a technical solution that can maximize the extracted power.

4 Effect of bypass diode

In recent years, a serious concern affecting PV modules is the partial shading condition because of difficulties such as shade due to buildings, trees, sand, and objects [17]. The outcomes of the PSC are the hot spot phenomenon in PV cells. Therefore, to protect the PV modules from the damaging effects of hot-spots, problems can be addressed by connecting each module with a bypass diode, as shown in Fig. 3. The PSC has a higher impact on decreasing the power of solar systems, which rely on the shading pattern, a number of bypass diodes, and the configuration of solar systems.

The shaded PV module acts as a load rather than a generator in that it becomes reverse biased and generates heat. This is called the hot-spot effect, and if this generated heat exceeds a certain limit, it then causes breakdown and damages the cell, becoming an open circuit. The bypass diode is inserted into the PV system, as shown in Fig. 3, to prevent such a dangerous situation. If the PV modules are exposed to normal conditions, the bypass diodes will be in the reverse cut-off state. If the PV modules are exposed to the PSC, the bypass diode conducts to form a short-circuit, preventing it from being reversed by the reverse leakage current and increasing the overall output power.

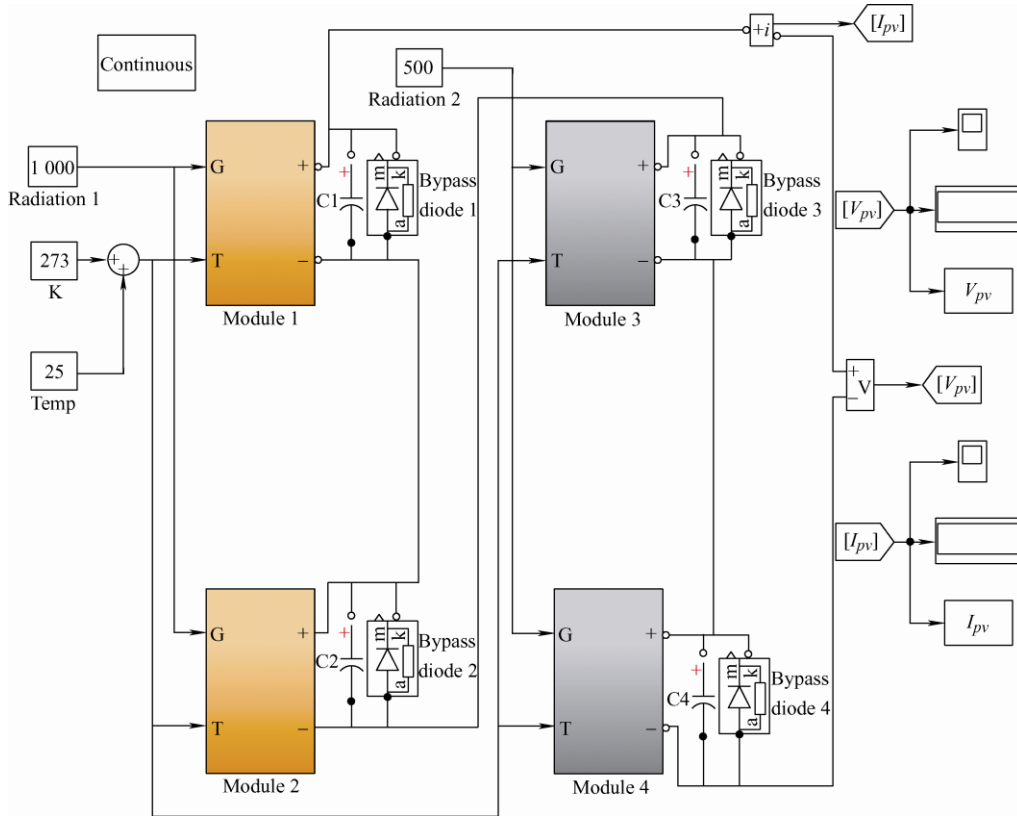


Fig. 3 Modeled subsystem of PV system under the condition of partial shading

5 DC-DC boost converter

DC-DC converters are extensively implemented in PV systems as a link device between the PV generating system and the consumers. In addition, they are used to match the process between the voltage of PV panels at the MPP and the load voltage. The main function of the DC-DC converter is to convert an input power $P_{in} = V_{in} \times I_{in}$ to $P_o = V_o \times I_o$ with the most feasible efficiency. The DC-DC converter is used to alter the input voltage level to a higher or lower level. Hence, the efficiency η of the DC-DC converter can be acquired from Eq. (2) as follows

$$\eta = \frac{P_o}{P_{in}} = \frac{V_o \times I_o}{V_{in} \times I_{in}} \tag{2}$$

As a result, the relationship between the output and input parameters can be calculated as in Eq. (3).

$$V_o \times I_o = \eta \times V_{in} \times I_{in} \tag{3}$$

The efficiency remains almost constant at specific values of the converter current and voltage. Any increments of V_{in} or I_{in} in Eq. (3) increase in either V_o or I_o . The DC-DC converter used in this work is a boost converter, which steps up the PV voltage level to a high output voltage level.

The block diagram in Fig. 4 shows the basic components of the boost converter. Boost converters are

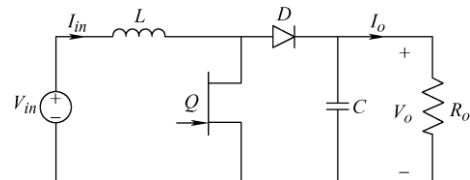


Fig. 4 Equivalent circuit of boost converter

used in applications that require that the input voltage be stepped up to a higher level. The voltage ratio can be calculated as shown in Eq. (4).

$$V_o/V_i = 1/(1 - D) \tag{4}$$

The duty cycle D in Eq. (4) varies between 0 and 1. This means that the voltage ratio is always greater than 1, which causes the converter to be used as a step-up converter^[18-19].

6 Particle swarm optimization

PSO is a search method that is based on the algorithm for improving population randomization, where the swarm can be retained for each individual particle to represent the candidate solution. The ideal solution for the problem is represented by the position

in the optimum particle space while the orientation of particles and the velocity value are determined by the particle's velocity vector, where each particle obeys the current optimal particle and searches the optimization in the solution are based on the experience of itself flying [20-22]. Although the PSO has some advantages, including robustness, flexibility, and rapidity, during the tracking process, it is easy for the MPP to fall into the local optimum, which causes a failure to attain the global peak.

The PSO scheme is mainly considered as an efficient technique for obtaining the global peak under the conditions of partial shadow. In Ref. [20], a genetic algorithm is used with the PSO to obtain a modified method that can find the global peak with faster tracking velocity and less oscillation than the unadjusted method. In Ref. [21], the predicted calculation is currently computed based on the output current of the solar power system in the PSC, after which the traditional PSO is executed to obtain the global maximum point. In Ref. [22], a voltage-based PSO method is proposed, where the DC voltage super-position principle is applied to obtain the output characteristics of PV systems, and the standard PSO method is then applied to obtain the global peak point. As a result, the PSO method is more robust and rapid in extracting the global peak compared to conventional methods, where the global peak of the PV curve can be extracted proficiently under any surrounding shading conditions.

6.1 Modified particle swarm optimization

In normal PSO, the part "particles" refers to population members, which have a small mass and small volume, and are subject to speeds or accelerations with the best performance. Every particle in the swarm represents a solution in a high-dimensional space with four vectors, which are: ① present position; ② after the acceleration of particles compared to the old position, it selected the personal best position of all particles; ③ particle speed; and ④ the global best position for all particles that have thus far originated in its neighborhood. Every particle regulates its position X_{ij} inside the limited search area based on the best position that is achieved by itself $X_{Pbest.ij}$ and the global best position

that is achieved by all particles $X_{Gbest.ij}$. Through the search procedure for bests that can be detailed with equations as follows [23].

6.2 Velocity step function

Conventional PSO employs step function V_{ij}^t , which is determined for every particle i th of every j th variable at every iteration t , where $V_{ij}^t \geq 0$, as seen in Eq. (5), refers to a three-part equation. To move from one position to another in the search area; particles are fixed by three mean the inertia function ω , which could be counted in every iteration from Eq. (6); the inertia operator limit values and the third term are the maximum fit iteration number t_{max} ; the second term refers to updating the present location's procedure, and the third represents the method of sharing information of the global best solution between old locations. Here, an important change is that global optimization should also guide the individual optimization to reach the optimal solution as the acceleration factor of the convergence process, which can be expressed mathematically using Eq. (7). Therefore, the other two changes made to the old speed function are c_1 , c_2 , c_3 , and c_4 , which are called constant parameters, and the random numbers of MPSO, r_1 , r_2 , r_3 , and r_4 , which are between [0, 1].

$$V_{ij}^{t+1} = \omega^t V_{ij}^t + c_1 r_1 (X_{Pbest.ij}^t - X_{ij}^t) + c_2 r_2 (X_{Gbest.i}^t - X_{ij}^t) \quad (5)$$

$$\omega^t = \omega_{max} - ((\omega_{max} - \omega_{min}) / t_{max}) \times t \quad \forall \omega \geq 0 \quad (6)$$

$$V_{ij}^{t+1} = V_{ij}^{t+1} + c_3 r_3 (X_{Gbest.j}^t + X_{Pbest.ij}^t - 2X_{ij}^t) + c_4 r_4 (X_{Gbest.i}^t - X_{Pbest.ij}^t) \quad (7)$$

6.3 Updating the i th particle position

Ever particle should transfer towards the optimum by properly updating its location utilizing the step function V_{ij}^t , as seen in Eq. (8), where the step is added to the present location. The step may be positive or negative until it becomes zero, after which it is the optimum solution

$$X_{ij}^{t+1} = X_{ij}^t + V_{ij}^{t+1} \quad (8)$$

6.4 Search space limit reduction strategy

Here, considering decreasing the search area to discover the optimum value, which is another

modification added to the searching process, which requires the adjustment and modification of the limits of the controlled variables in each iteration. Therefore, for the X_i controlled variable, the limit is modified in a reducing way to make it converge to the global best location in every iteration compared to its old limit. The limit reduction strategy (LRS) could be deduced mathematically using Eqs. (9) and (10).

$$X_{i,\max}^{t+1} = X_{i,\max}^t - \sigma(X_{i,\max}^t - X_{Gbest,i}^t) \quad (9)$$

$$X_{i,\min}^{t+1} = X_{i,\min}^t - \sigma(X_{Gbest,i}^t - X_{i,\min}^t) \quad (10)$$

where σ is a factor that is less than 0.1; depending on the problem, it is selected randomly and adjusted.

6.5 Velocity limit control

The last modification here is that the velocity step or step length is limited according to the maximum/minimum values of controlled variables X_i^{\max} , X_i^{\min} which is suitable when moving to the achieved optimum solution. The velocity limits V_i^{limits}

may be revised according to each circumstance or system with an appropriate choice of the value of the velocity limit operator β given as in Eq. (11)

$$V_i^{limits} = \pm\beta(X_i^{\max} - X_i^{\min}) \quad (11)$$

6.6 Combination of MPSO and studied problem

This section shows how the optimization handles PV system difficulties, in other words, defining the PV system difficulties-controlled variables and objective function and system constraints. In addition, the optimization technique described above is now performed on an MPPT controller for the PV system under consideration, which operates under the PSC. Fig. 5 shows the flowchart of the complete implementation process of the proposed work using MPSO. Here, a particle's position is taken as the duty ratio (d) of the converter, and the fitness value of a particle is the generated PV power P_{pv} of the whole PV system.

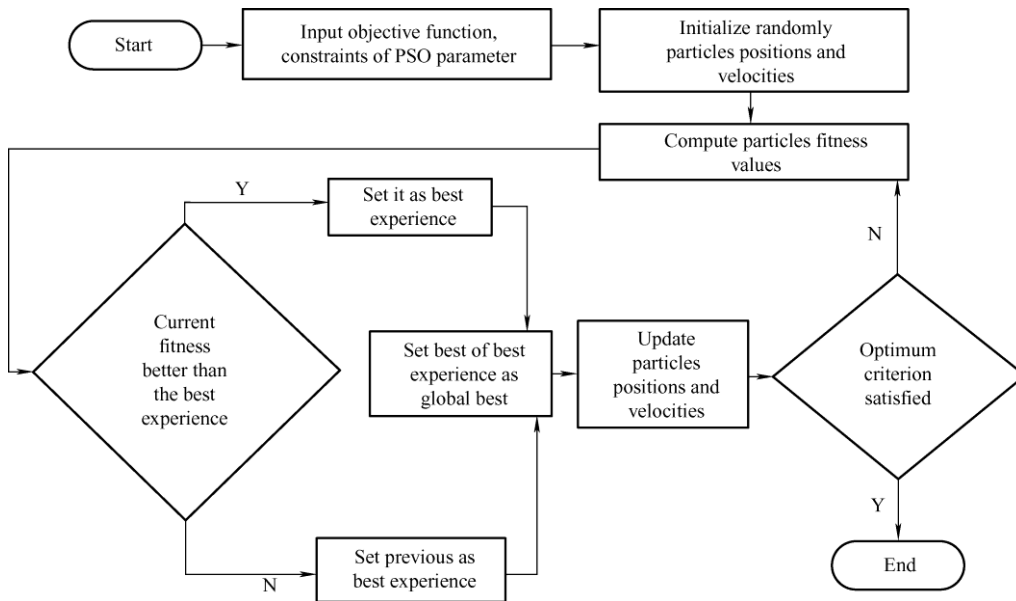


Fig. 5 Particle swarm optimization process flowchart

For a DC-DC power converter, if the output voltage is constant, the input voltage (PV output voltage) can be calculated from the output voltage V_o and the duty cycle (d). For instance, for the step-up converter used in this thesis, the input voltage can be calculated as follows

$$V_{in} = V_o \times (1-d) \quad (12)$$

Therefore, to execute the PSO algorithm for PV systems, the particle position (X_{ij}^t) in Eqs. (5)-(7) can

be measured as the duty cycle d_{ij}^t of the PV converter, while the velocity (V_{ij}^t) can be measured as the variation of the duty cycle Δd_{ij}^t .

The variation of the duty cycle Δd_{ij}^t is influenced by two variables, the best solution obtained by the particle itself (P_{best}), and the best solution in the whole population (G_{best}). If the present duty cycle d_{ij}^t is not obtained from these two values, and it will be updated using a high velocity. When the condition in Eq. (14) is satisfied, P_{best} in Eq. (13) will be updated; otherwise,

P_{best} maintains its current value. Then, the fitness value of every particle will be estimated to see if the G_{best} value requests to be updated.

$$P_{best} = d_{ij}^t \quad (13)$$

$$f(d_{ij}^t) = f(P_{best}) \quad (14)$$

where f is the objective function that should be improved.

6.7 Procedure for PSO algorithm

Step 1: Initialization. At the primary stage, PSO generates particles randomly in the search area.

Step 2: Evaluation of fitness. Estimate the fitness value of every particle by transferring the candidate solution to the objective function.

Step 3: Choose the personal best and global best

solution. Discover the particles' own best solution and global best solution amongst all particles.

Step 4: Update the location and speed of each particle.

Estimate the new location and speed of every particle.

Step 5: Conclusion of convergence. Re-initialize the PSO algorithm if the constraint is not met. In other words, the algorithm stops when the G_{best} starts.

7 Simulation results and discussion

Matlab/Simulink is one of the significant tools which are used to determine the performance (robustness and effectiveness) of the recommended MPPT algorithm. The modeling of PV system with a boost converter and MPPT algorithms was done in the Matlab, which is shown in Fig. 6.

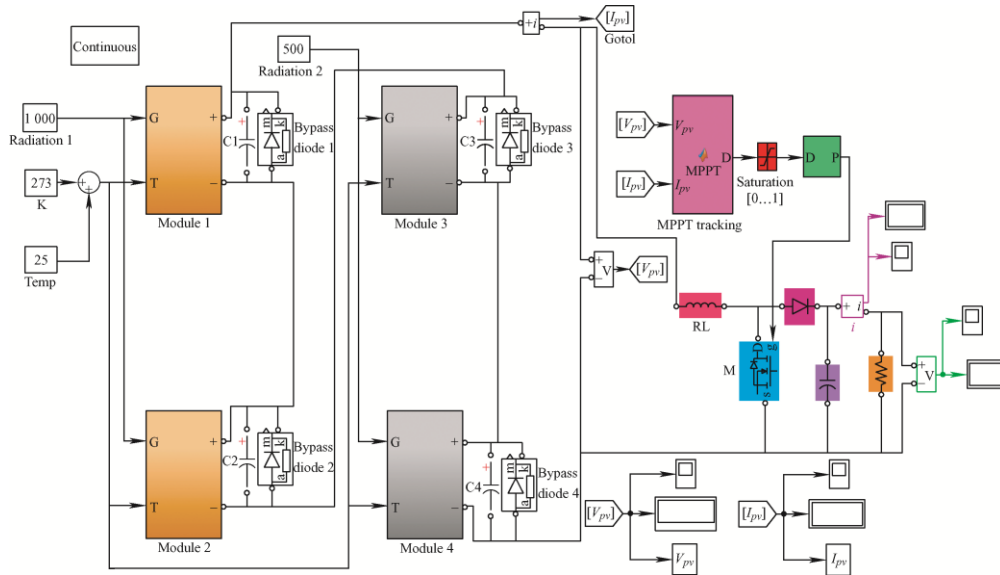


Fig. 6 Matlab/Simulink model of ANN and PSO MPPT system

The parameters of the PV system, DC-DC boost converter and, PSO algorithm are listed in Tabs. 1-3 [14, 23]. A comparative analysis of the proposed system was done with the actual values, ANN, and PSO algorithm under environmental conditions.

Tab. 1 Detail of PV module

Parameter	Value
Maximum power P_m/W	250
Maximum power voltage V_m/V	30.2
Maximum power current I_m/A	8.28
Open-circuit voltage V_{oc}/V	36.0
Short-circuit current I_{sc}/A	8.56
Number of series modules N_s	4
Number of cells per module N_{cell}	60

Tab. 2 PSO algorithm parameters

Parameter	Value
Populations size P	300
Inertia weight ω	0.4
Constants (c_1, c_2, c_3, c_4)	1.3, 2, 10, 0.002 5
Velocity limit operator β	0.1
Generations (Iterations) t	300
LRS operator σ	0.1

Tab. 3 Specifications of DC-DC boost converter

Parameter	Value
Inductance L/mH	1.147 8
Capacitance C/mF	0.467 6
Load resistance/ Ω	100
Switching frequency/kHz	50

The PV experimental platform that was used as a reference to design the proposed system is shown in Fig. 7.



Fig. 7 Platform of experimental PV lab

The first simulation was performed to produce the characteristic curves of the PV array under uniform and non-uniform weather conditions, where the PV array is not connected to the boost converter or MPPT algorithms. Therefore, many cases of PV arrays under the PSC were also tested in the first simulation. For the second simulation, PV modules connected to the boost converter and MPPT algorithms, which were tested under uniform and non-uniform weather conditions and the corresponding maximum power, voltage, and current generated by the PV array under different combinations of solar irradiance according to the configuration presented in Tab. 4. In addition, many cases were examined for comparison between the actual results of the experimental platform and the MPPT algorithms (MPSO and ANN). Six cases are listed in Tab. 4 to show that MPSO is better than ANN in the field of MPPT of PV systems.

The P-V characteristics of the PV array under uniform and non-uniform weather conditions are shown in Fig. 8. All PV modules were exposed under full radiation for Case 1; hence, there was only one

MPP generated at 1 000 W, while another three cases of PV modules were exposed under the PSC for Cases 2, 3, 4, 5, and 6. All six cases were tested and presented to explain and distinguish between the global peak of local peaks, which is given in Fig. 8. The P-V characteristic curves show that three peaks were established for Cases 2, 3, and 4 because the PV arrays were partially shaded by three different solar irradiances values, where the global MPP for the 2, 3, and 4 cases are (701.8, 433.4, and 942.8, respectively). In addition, four peaks were established for Cases 5 and 6 because the PV arrays were partially shaded by four different solar irradiance values, where the global MPP for the 5 and 6 cases are (708.3 and 561.2).

In scenario 1, the PV system is exposed to the same levels of irradiation and under uniform radiations conditions (1 000, 1 000, 1 000, and 1 000 W/m²) and one constant temperature (25 °C) as presented in Fig. 8a, where the PV curve has one global peak (1 000 W). Meanwhile, Fig. 9 shows a comparison of the power and voltage for both MPSO and ANN with the measured value of the lab experiment platform, and it shows that the proposed MPPT method (MPSO) can track the actual maximum power (1 000) efficiently under uniform radiation conditions. The MPSO-based MPPT method provided P_{\max} , V_{\max} , and I_{\max} data points that match data points measured from the actual Simulink model with respect to the lab experiment platform. Further, the output of MPSO is better than the output of the ANN controller under uniform weather conditions. Finally, the global maximum power point is effectively extracted using the MPSO tracker within a short period compared to the ANN method.

In scenario 2, the PV system is exposed to nonuniform levels of irradiation and PSCs (1 000, 900, 500, and 1 000 W/m²) and one constant temperature (25 °C), as shown in Fig. 8b, where the PV curve has several local peaks and one global peak (701.8 W), which the MPPT trackers need to track and achieve this global peak.

Fig. 10 displays the output power and voltage for all of the MPSO, ANN, and actual values, which indicates that the proposed MPPT method (MPSO) is capable of efficiently tracking the actual maximum

power under nonuniform levels of irradiation and PSCs. The MPSO-based MPPT method provides the data points P_{max} , V_{max} , and I_{max} , which match the measured data points obtained from the actual

Simulink model with respect to the lab experiment platform. In addition, the output of MPSO is better than the output of the ANN controller under the PSD and non-uniform irradiation levels.

Tab. 4 Irradiance data input, ANN, and PSO output data power and voltage

Cases	Radiations				$P_{max-Actual}/W$	$P_{max-MPSO}/W$	$P_{max-ANN}/W$	$V_{max-MPSO}/V$	$V_{max-ANN}/V$
	PV 1	PV 2	PV 3	PV 4					
Case 1	1 000	1 000	1 000	1 000	1 000.0	998.7	725.9	316.0	269.4
Case 2	1 000	900	500	1 000	701.8	698.9	559.7	264.4	236.6
Case 3	1 000	400	600	400	433.4	421.0	302.8	205.2	174.0
Case 4	900	1 000	1 200	900	942.8	939.0	723.3	306.2	268.9
Case 5	500	800	1 200	650	561.2	552.1	547.2	235.0	233.9
Case 6	700	1 000	650	900	708.3	681.1	560.1	261.0	236.7

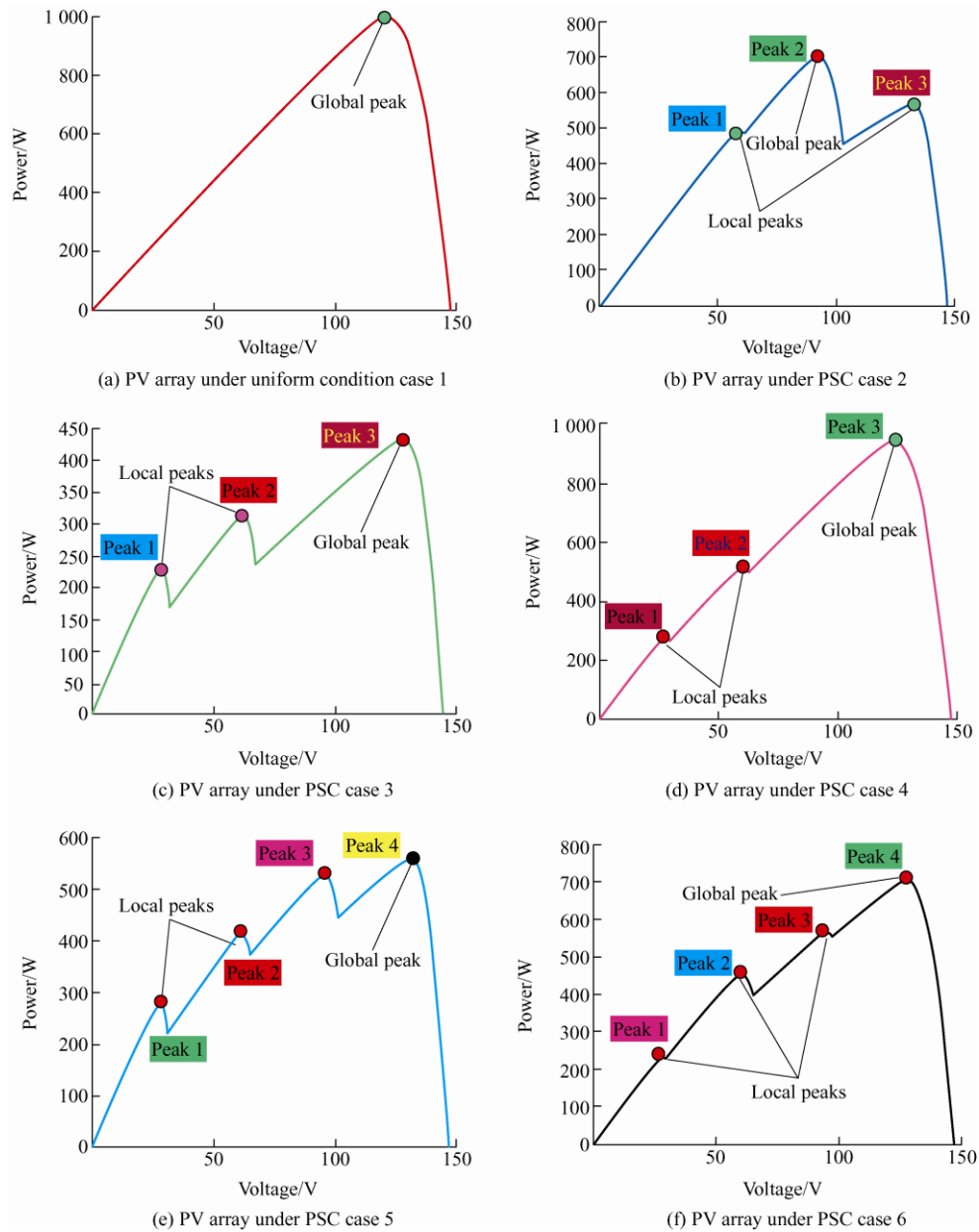


Fig. 8 P-V characteristics of the PV array under uniform and non-uniform weather conditions

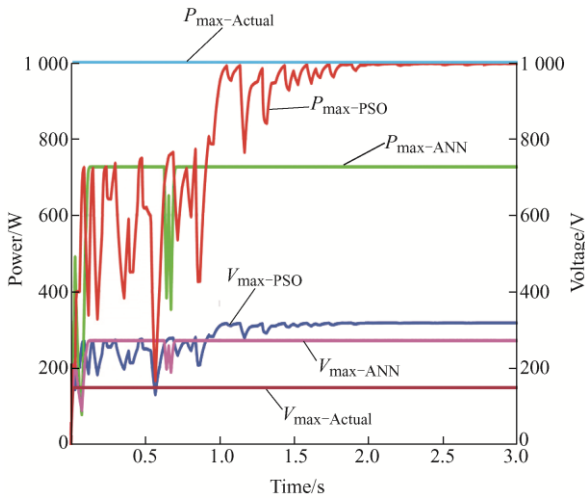


Fig. 9 Comparison of P_{MPP} , V_{MPP} , and the actual values for both the MPSO and ANN for scenario 1

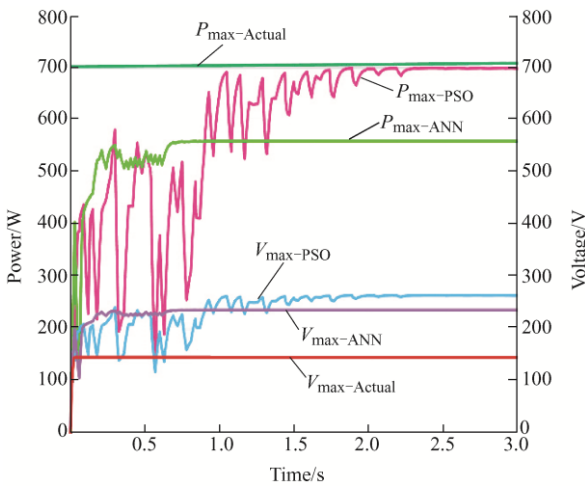


Fig. 10 Comparison of P_{MPP} , V_{MPP} , and the actual values for both the MPSO and ANN for scenario 2

In scenario 3, the PV system is exposed to nonuniform levels of irradiation and PSCs (1 000, 400, 600, and 400 W/m^2) and one constant temperature (25 $^{\circ}C$). As presented in Fig. 8c, the P-V curve has various local peaks and one global peak (433.4 W), which the MPPT trackers are supposed to track to find this GP.

Fig. 11 shows the output power and voltage for all the MPSO, ANNs, and actual values. Moreover, it shows that the proposed MPPT method (MPSO) can efficiently track the actual maximum power under nonuniform levels of irradiation and PSCs. The MPSO-based MPPT method gives P_{max} , V_{max} , and I_{max} values that are very close to the measured values obtained from the actual Simulink model with respect to the lab experiment platform.

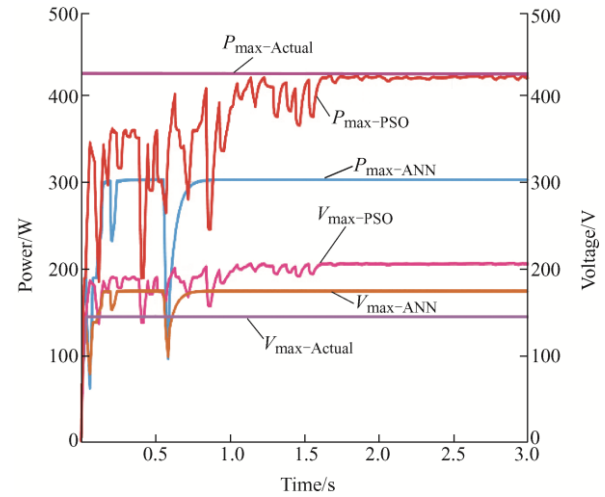


Fig. 11 Comparison of P_{MPP} , V_{MPP} , and the actual values for both the MPSO and ANN for scenario 3

In scenario 4, the PV system is exposed to the PSCs for which the radiations level are (1 000, 400, 600, and 400 W/m^2) and one constant temperature (25 $^{\circ}C$), which are seen in Fig. 8d. The P-V curve has various local peaks and one global peak (433.4 W), which the MPPT trackers are supposed to track to obtain this GP.

Fig. 12 shows the output power and voltage for all the MPSOs, ANNs, and actual values. Furthermore, it shows that the proposed MPPT method (MPSO) is intelligent and able to track the actual maximum power under PSCs. The MPSO-based MPPT method has P_{max} , V_{max} , and I_{max} values that are clearly close to the measured values obtained from the actual Simulink model with respect to the lab experiment platform.

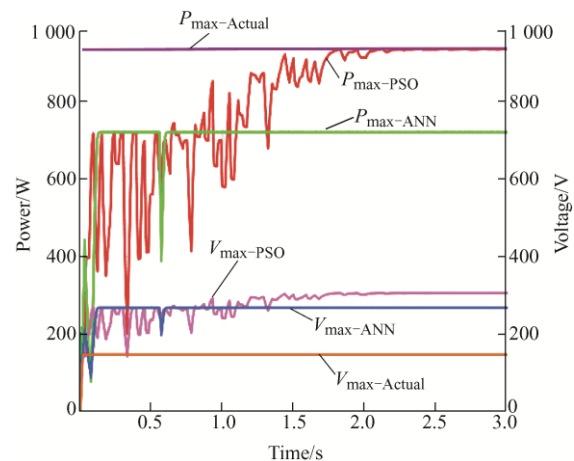


Fig. 12 Comparison of P_{MPP} , V_{MPP} , and the actual values for both the MPSO and ANN for scenario 4

In scenario 5, the PV system is exposed to nonuniform levels of irradiation and PSCs (500, 800, 1 200, and 650 W/m^2) and one constant temperature

(25 °C). As shown in Fig. 8e, the P-V curve has various local peaks and one global peak (561.2 W), which the MPPT trackers are supposed to track to find this GP.

Fig. 13 presents the output power and voltage for all the MPSO, ANNs, and actual values. Moreover, it shows that the proposed MPPT method (MPSO) can efficiently track the actual maximum power under nonuniform levels of irradiation and PSCs. Moreover, the proposed system has been tested under four peaks (global and local) and can distinguish between the global peak of local peaks.

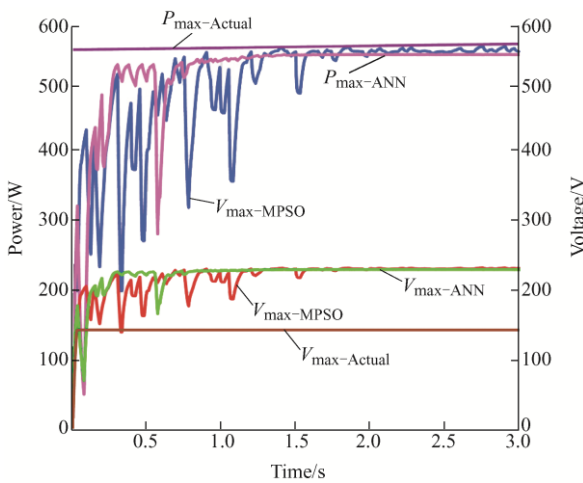


Fig. 13 Comparison of P_{MPP} , V_{MPP} , and the actual values for both the MPSO and ANN for scenario 5

In scenario 6, the PV system is exposed to nonuniform levels of irradiation and PSCs (700, 1 000, 650, and 900 W/m²) and one constant temperature (25 °C). As shown in Fig. 8e, the P-V curve has various local peaks and one global peak (708.3 W), which the MPPT trackers are supposed to track to find this GP.

Fig. 14 shows the output power and voltage for all the MPSO, ANNs, and actual values. Moreover, it shows that the proposed MPPT method (MPSO) can efficiently track the actual maximum power under nonuniform levels of irradiation and PSCs. Moreover, the proposed system has been tested under four peaks (global and local), and it can distinguish between the global peak of local peaks.

The efficiency is an important principle that is utilized to assess the performance of the MPPT model, which is found by the equation below

$$\eta = 1 - \frac{P_{\max\text{-Actual}} - P_{\max\text{-MPPT}}}{P_{\max\text{-Actual}}} \times 100\% \quad (15)$$

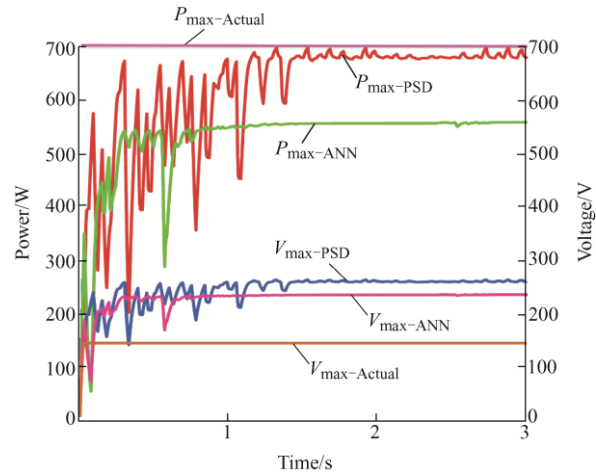


Fig. 14 Comparison of P_{MPP} , V_{MPP} , and the actual values for both the MPSO and ANN for scenario 6

The results of the efficiency study are presented in Tab. 5 and show that the simulation is based on the performance study MPPT technique under observation. It is observed that the irradiance value changes from 400 to 1 200 W/m², and the temperature remains the same for all four modules (25 °C).

Tab. 5 Performance efficiency for the MPSO and ANN

Cases	$P_{\max\text{-Actual}}$ /W	$P_{\max\text{-MPSO}}$ /W	Efficiency of MPSO(%)	$P_{\max\text{-ANN}}$ /W	Efficiency of ANN(%)
Case 1	1 000.0	998.7	99.870	725.9	72.590
Case 2	701.8	698.9	99.586	559.7	79.752
Case 3	433.4	421.0	97.139	302.8	69.866
Case 4	942.8	939.0	99.597	723.3	76.718
Case 5	561.2	552.1	98.378	547.2	97.505
Case 6	708.3	681.1	96.160	560.1	79.076

Regardless of the irradiation, the proposed MPSO performs effectively, which can be seen from Tab. 4. From the figures above, we can determine that the MPSO is near to the GMPP. The efficiency of the MPSO achieved with the least number of steady-state oscillations is 99%, which demonstrates that PSO is better in uniform and non-uniform irradiance conditions or PSCs.

As mentioned previously, there is a variety of techniques to determine the MPP under PSCs based on modified conventional methods, and smart methods have been developed in different studies, such as modified traditional methods, PSO, the Fibonacci line

search method, ANN technology, and Cuckoos' behavior method. It can be observed that there are

some differences in the real tracking mode, as presented in Tab. 6.

Tab. 6 Comparison between different tracking techniques under the partial shading conditions

Method	Tracking mode	Speed	Advantages	Disadvantages
Modified conventional methods ^[24-26]	In the first stage, a normal program is executed, then the adjacent is scanned during the second stage.	Normal	Easily applied	Large vibration and unstable output
Modified particle swarm optimization	A typical swarm intelligence algorithm, a candidate solution is signified by every particle, and the optimal solution of the problem is denoted by the particle position in the ideal space.	Fast	Swift tracking speed and very robust.	Complex calculation, and it is easy for the MPP to decrease to the local optimum, which causes a failure of the GP tracking
Fibonacci line search ^[27-28]	The horizon of searching is iteratively restricted and shifted.	Slow	Easily applied	Complex calculation
Artificial neural network ^[29-31]	The training process is complicated, and is totally based on experimental measurements.	Slow	Can be trained offline and applied in the on-line environment	Difficult computation
Cuckoos' behavior method ^[32-35]	It is similar to particle swarm optimization, and depends on the population algorithm.	Fast	Rapid convergence and effective randomization	Complex calculation, and failure of both solution quality and convergence velocity

The above discussions and results conclude that the modified PSO technique can track the actual maximum power regardless of the shading conditions and scenarios. For all considered shading scenarios, it was observed that the proposed method can easily track the actual maximum power for an UP-S250 PV array system. In addition, under non-uniform irradiation conditions for all scenarios, it can be shown that the proposed technique exhibits a rapid response and good stabilization at the actual MPP, and the global MPPT can be tracked rapidly with an efficiency of almost 99% for all investigated scenarios, as shown in Fig. 15. Further, it can be applied to solve engineering problems.

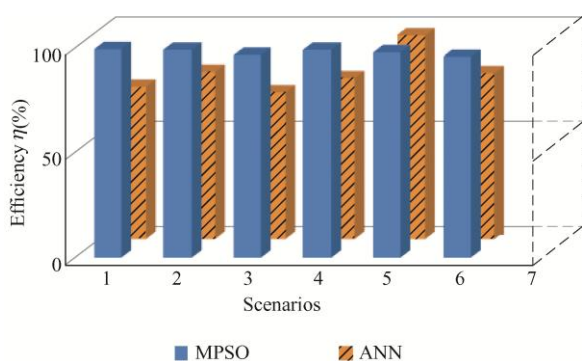


Fig. 15 Comparison efficiency

8 Conclusions

An important objective of MPPT methods is that they are primarily used in practice to obtain the maximum power of PV systems and to provide this

power to the consumer load. When the PV system is influenced by uniform solar irradiation, the characteristic of the system will be nonlinear with only one MPP, which can be easily obtained using a simple control technique, such as perturb and observe, modified perturb and observe, and incremental conductance (INC). Conversely, in the case of non-uniform solar irradiation conditions, the characteristic curve of the PV system will have multiple MPPs, which are visible owing to the connection of bypass diodes to each PV module that is connected to eliminate the effect of hot spots. The existence of these multiple peaks on the characteristic curves of PV systems has motivated researchers to design a more suitable method that can distinguish between each peak point on the P-V curve, thus enabling the determination of the accurate maximum power for delivery to the load.

The main work of this study and the results achieved are as follows.

(1) Proposed an effective MPPT-tracking method to predict the global maxima power point (GMMP) of a PV system under all conditions of the surrounding weather either under normal conditions, such as uniform irradiation conditions or under abnormal conditions, such as partial shading conditions.

(2) A database has been obtained from the experiment platform for analysis, and it was used to train the MPSO and ANN. The MPSO and ANN were proposed by using two inputs (the PV system voltage

and current) and one output (the duty cycle). The MPSO generated the desired duty cycle, which gives the desired maximum voltage accordingly.

(3) The proposed method was studied under different scenarios involving partial shading levels to determine its effectiveness. The proposed technique was shown to effectively and robustly track the global maximum power as required. The proposed scheme has an excellent tracking performance in terms of efficiency and stability, as shown by the simulation results.

References

- [1] N A Ahmed, M Miyatake. A novel maximum power point tracking for photovoltaic applications under partially shaded insolation conditions. *Electric Power System Research*, 2008, 78(5): 777-784.
- [2] M Oulcaid, H E Fadil, A Yahya, et al. Maximum power point tracking algorithm for photovoltaic systems under partial shaded conditions. *IFAC-Papers OnLine*, 2016, 49(13): 217-222.
- [3] M Miyatake, M Veerachary, F Toriumi, et al. Maximum power point tracking of multiple photovoltaic arrays: A PSO approach. *IEEE Transactions on Aerospace and Electronic Systems*, 2011, 47(1): 367-380.
- [4] S R Chowdhury, H Saha. Maximum point tracking of partially shaded solar photovoltaic arrays. *Solar Energy Material and Solar Cells*, 2010, 94(9): 1441-1447.
- [5] M Seyedmahmoudian, T K Soon, B Horan, et al. New ARMO-based MPPT technique to minimize tracking time and fluctuation at output of PV systems under rapidly changing shading conditions. *IEEE Transactions on Industrial Informatics*, 2019. DOI: 10.1109/TII.2019.2895066.
- [6] K S Tey, S Mekhilef, M Seyedmahmoudian, et al. Improved differential evolution-based MPPT algorithm using SEPIC for PV systems under partial shading conditions and load variation. *IEEE Transactions on Industrial Informatics*, 2018, 14(10): 4322-4333.
- [7] M Seyedmahmoudian, B Horan, T K Soon, et al. State of the art artificial intelligence-based MPPT techniques for mitigating partial shading effects on PV systems: A review. *Renewable and Sustainable Energy Reviews*, 2016, 64: 435-455.
- [8] T Radjai, J P Gaubert, L Rahmani, et al. Experimental verification of P&O MPPT algorithm with direct control based on Fuzzy logic control using CUK converter. *International Transactions on Electrical Energy Systems*, 2015, 25(12): 3492-3508.
- [9] T Radjai, L Rahmani, S Mekhilef, et al. Implementation of a modified incremental conductance MPPT algorithm with direct control based on a fuzzy duty cycle change estimator using dSPACE. *Solar Energy*, 2014, 110: 325-337.
- [10] K S Tey, S Mekhilef. Modified incremental conductance MPPT algorithm to mitigate inaccurate responses under fast-changing solar irradiation level. *Solar Energy*, 2014, 101: 333-342.
- [11] K S Tey, S Mekhilef. Modified incremental conductance algorithm for photovoltaic system under partial shading conditions and load variation. *IEEE Transactions on Industrial Electronics*, 2014, 61(10): 5384-5392.
- [12] A Safari, S Mekhilef. Simulation and hardware implementation of incremental conductance MPPT with direct control method using cuk converter. *IEEE transactions on industrial electronics*, 2010, 58(4): 1154-1161.
- [13] T K Soon, S Mekhilef. A fast-converging MPPT technique for photovoltaic system under fast-varying solar irradiation and load resistance. *IEEE transactions on industrial informatics*, 2014, 11(1): 176-186.
- [14] M B Shafik, H Chen, G I Rashed, et al. Adequate topology for efficient energy resources utilization of active distribution networks equipped with soft open points. *IEEE Access*, 2019, 7: 99003-99016.
- [15] F Li, Y Huang, F Wu, et al. Research on clustering equivalent modeling of large-scale photovoltaic power plants. *Chinese Journal of Electrical Engineering*, 2018, 4(4): 80-85.
- [16] Y Zhang, J Xiong, P He, et al. Review of power decoupling methods for micro-inverters used in PV systems. *Chinese Journal of Electrical Engineering*, 2018, 4(4): 26-32.
- [17] S Silvestre, A Boronat, A Chouder. Study of bypass diodes configuration on PV modules. *Applied Energy*, 2009, 86(9): 1632-1640.
- [18] A W Ibrahim, M Ding, X Jin, et al. Artificial neural network based maximum power point tracking for PV system. *Chinese Control Conference(CCC)*, 27-30 July, 2019, Guangzhou, China. IEEE, 2019: 6559-6564.
- [19] R Abid, F Masmoudi, F B Salem, et al. Modeling and simulation of conventional DC-DC converters dedicated to photovoltaic applications. In *7th International Renewable Energy Congress (IREC)*, 22-24 March, 2016, Hammamet, Tunisia. IEEE, 2016: 1-6.
- [20] L Liu, Z Liu. A novel combined particle swarm optimization and genetic algorithm MPPT control method

- for multiple photovoltaic arrays at partial shading. *Journal of Energy Resources Technology*, 2013, 135(1): 52-56.
- [21] L Liu, C Liu, H Gao. A novel improved particle swarm optimization maximum power point tracking control method for photovoltaic array by using current calculated predicted arithmetic under partially shaded conditions. *Journal of Renewable and Sustainable Energy*, 2013, 5(6): 1613-1622.
- [22] H Li, L Liu. A novel PSO MPPT control method based on DC voltage super-position principle under partially shaded conditions. *Journal of Vibration and Control*, 2014, 20(6): 1356-1360.
- [23] M B Shafik, H Chen, G I Rashed, et al. Adaptive multi objective parallel seeker optimization algorithm for incorporating TCSC devices into optimal power flow framework. *IEEE Access*, 2019, 7: 36934-36947.
- [24] H Patel, V Agarwal. Maximum power point tracking scheme for PV systems operating under partially shaded conditions. *IEEE Transactions on Industrial Electronics*, 2008, 25(4): 1689-1698.
- [25] G Carannante, C Fraddanno, M Pagano, et al. Experimental performance of MPPT algorithm for photovoltaic sources subject to inhomogeneous insolation. *IEEE Transactions on Industrial Electronics*, 2009, 26(11): 4374-4380.
- [26] E Koutroulis, F Blaabjerg. A new technique for tracking the global maximum power point of PV arrays operating under partial-shading conditions. *IEEE Journal of Photovoltaics*, 2012, 2(2): 184-190.
- [27] A A Nabil, M Masafumi. A novel maximum power point tracking for photovoltaic applications under partial shaded insolation conditions. *Electric Power System Research*, 2008, 78(5): 777-784.
- [28] R Ramaprabha, M Balaji, B L Mathur. Maximum power point tracking of partially shaded solar PV system using modified Fibonacci search method with fuzzy controller. *Electric Power and Energy System*, 2012, 43(1): 754-765.
- [29] E Syafaruddin, E Karatepe, T Hiyama. Artificial neural network-polar coordinated fuzzy controller based maximum power point tracking control under partially shaded conditions. *IET Renewable Power Generation*, 2009, 3(2): 239-253.
- [30] E Syafaruddin, K Hiyama. Fuzzy wavelet network identification of optimum operating point of non-crystalline silicon solar cells. *Computer and Mathematics with Application*, 2012, 63(1): 68-82.
- [31] K Punitha, D Devaraj, S Sakthivel. Artificial neural network based modified incremental conductance algorithm for maximum power point tracking in photovoltaic system under partial shading conditions. *Energy*, 2013, 62: 330-340.
- [32] A Jubaer, S Zainal. A maximum power point tracking, MPPT for PV system using Cuckoo search with partial shading capability. *Applied Energy*, 2014, 119: 119-130.
- [33] L Tarik, A Aouatif, R Mohammad. A hybrid mobile object tracker based on the modified Cuckoo search algorithm Kalman filter. *Pattern Recognition*, 2014, 47(11): 3597-3613.
- [34] M F Shlesinger, J Klafter. Levy walks versus Levy flights. *On Growth and Form*. Dordrecht: Martinus Nijhof Publisher, 1986, 279-283.
- [35] X Yang, S Deb. Engineering optimization by Cuckoo search. *International Journal of Mathematical Modeling and Numerical Optimization*, 2010, 1(4): 330-343.



Al-wesabi Ibrahim was born in IBB, Yemen, in 1988. He received the B.S. degree in electrical power and machines engineering from Sana'a University; Yemen, in 2014, and the master's degree in control science and engineering from the China University of Geoscience, Wuhan, China, in 2020. He is currently a Ph.D. candidate at the School of

Electrical Engineering and Automation, China University of Geoscience, Wuhan, China. His research interests include smart electric grids, MPPT controllers for PV systems, machine learning, automation systems, and optimization.



M.B. Shafik was born in Kafrelsheikh, Egypt, in 1986. He received a B.S. degree in electrical power and machines engineering from Kafrelsheikh University, Egypt, in 2008, and master's degree in electrical power engineering from Tanta University, Egypt, in 2013. He is currently a Ph.D. candidate at the School of

Electrical Engineering and Automation, Wuhan University, Wuhan, China. His research interests include smart electric grids, active distribution networks, planning, Internet of Things, automation systems, and optimization.



Min Ding received the B.S. degree in automation in 2009, and the M.S. in control science and control engineering in 2011 from Central South University, Changsha, China. She received the Ph.D. degree from the Graduate School of Environment and Energy Engineering, Waseda University, Tokyo, Japan. She is currently a lecturer with the School of

Automation at the China University of Geosciences, Wuhan, China. Her research interests include renewable energy generation and control, microgrid control and operation optimization, wind power prediction, and user behavior analysis, including distributed generation.



Mohammad Abu Sarhan received an M.S. degree in control science and engineering from China University of Geosciences, Wuhan, China, in 2019. He is currently working in the sector of electrical power engineering and renewable energy resources in the MENA region. His research interests include the areas of smart grids, renewable energy, and

electrical power systems.



Zhijian Fang (M'13) was born in Nanzhang, Hubei, China, in 1988. He received the B.S. and Ph.D. degrees in electrical engineering from Huazhong University of Science and Technology, Wuhan, China, in 2010 and 2015, respectively. Since 2018, he has been a professor with the School of Automation, China University of Geosciences, Wuhan,

China. From July 2015 to November 2018, he was a lecturer with the School of Electrical Engineering and Automation, Wuhan University, China. From February 2016 to January 2017, he was a post-doctoral research fellow with the Department of Electrical and Computer Engineering, Ryerson University, Canada. His research interests include high-performance DC/DC converters, battery chargers, renewable energy applications, and wireless power transfer.



Ahmed. G. Alareqi was born in Taiz, Yemen, in 1989. He received the B.S. degree in 2012 from Aden University, Faculty of Oil and Minerals, Yemen, in Oil and Natural Gas Engineering, and a master's degree in Oil and Natural Gas Engineering from the China University of Geosciences Wuhan, China, in 2019, and he is now a Ph.D. scholar at the School of Oil and Natural Gas Engineering, China University of

Geosciences, Wuhan, China. His research interests include drilling and applied technology, to optimize and enhance drilling efficiency to achieve the optimal rate of penetration, especially in basement rock drilling.



Tariq Al'moqri received a B.S. degree in Mathematics from Tamar University, Yemen, in 2010. He is currently pursuing an M.S degree in applied mathematics at China University of Geosciences, Wuhan, China. His research interests are around data mining, machine learning, and optimization.



Ayman. M. Al-Rassas was born in Ibb, Yemen, in 1989. He received his B.S in petroleum engineering, in 2015, from USCI University, Malaysia. He received his master's degree in Oil and Natural Gas Engineering, from Faculty of Earth Resources, China University of Geosciences, Wuhan, China. Currently, he is doing his Ph.D. in oil-gas field development engineering at China University of Petroleum (East China), and his current research is about

CO₂-EOR, unconventional resources.